1216 *Inorg. Chem.* **1993,** *32,* 1216–1221

ESR Characterization of *trans*-$V^{II}(py)_4X_2$ and *trans*-$Mn^{II}(py)_4X_2$ (X = NCS, Cl, Br, I; py = Pyridine)[§]

Claus J. H. Jacobsen,*,†,‡ Erik Pedersen,‡ Jørgen Villadsen,*,‡ and Høgni Weihe*,†

Haldor Topsøe Research Laboratories, Haldor Topsøe A/S, Nymøllevej 55, DK-2800 Lyngby, Denmark, and Department of Inorganic Chemistry, H. C. Ørsted Institute, University of Copenhagen, Universitetsparken 5, DK-2100 Copenhagen Ø, Denmark

Received July 1, 1992

Compounds having the general formula *trans*-$M^{II}(py)_4X_2$ (M^{II} = V, Mn, Fe, Co, Ni, Ru; X = NCS, Cl, Br, I) have been synthesized, and the vanadium(II) and manganese(II) compounds have been characterized by ESR spectroscopy using the iron, cobalt, nickel, and ruthenium compounds as solid solvents. Furthermore, all compounds prepared have been characterized by means of X-ray powder diffraction and thereby space groups and unit cell parameters have been obtained in most cases. The spin-Hamiltonian parameters have been obtained for all the V^{II} and Mn^{II} compounds using a simulation procedure involving exact numerical diagonalization of the spin-Hamiltonian matrices. It was found that the paramagnetic *trans*-$Fe(py)_4X_2$ and *trans*-$Co(py)_4X_2$ could be satisfactorily used at room temperature as solid solvents for the V^{II} and Mn^{II} compounds with respect to the ESR measurements, while this was not the case for the *trans*-$Ni(py)_4X_2$ compounds. This has been attributed to the orbitally degenerate ground states of iron(II) and cobalt(II). The *trans*-$Ru(py)_4X_2$ compounds, being diamagnetic, were also satisfactory solid solvents. The spin-Hamiltonian parameters obtained were found to be almost independent of the solid solvent, and typical values of the zero-field splitting parameters for the vanadium(II) compounds were for *trans*-$V(py)_4(NCS)_2$ and *trans*-$V(py)_4Cl_2$, $|D| \approx 0.2$ cm^{-1}, and for *trans*-$V(py)_4Br_2$ and *trans*-$V(py)_4I_2$, $|D| \approx 0.37$ cm^{-1}, and for the manganese(II) compounds, *trans*-$Mn(py)_4(NCS)_2$, $|D| \approx 0$ cm^{-1}, *trans*-$Mn(py)_4Cl_2$, $|D| \approx 0.2$ cm^{-1}, *trans*-$Mn(py)_4Br_2$, $|D| \approx 0.65$ cm^{-1}, and *trans*-$Mn(py)_4I_2$, $|D| \approx 0.95$ cm^{-1}. In all cases except *trans*-$Mn(py)_4(NCS)_2$ the rhombic zero-field splitting parameter E was found to be low ($<{}^1/_{10}D$). The g values of the vanadium(II) and manganese(II) compounds were 1.98 and 2, respectively, and the hyperfine coupling constants were 66.0×10^{-4} cm^{-1} $\leq |A| \leq 70.0 \times 10^{-4}$ cm^{-1} and $77.0 \times 10^{-4} \leq |A|\ 83.0 \times 10^{-4}$ cm^{-1}. These parameters are discussed in relation to the structures and compared to the parameters previously reported for the *trans*-$Cr(py)_4XY^+$ compounds which are isoelectronic with the corresponding vanadium(II) compounds. This study is the first systematic characterization of a series of vanadium(II) compounds by means of ESR spectroscopy, and to our knowledge it contains the hitherto most extensive nonapproximative simulations of ESR spectra.

Introduction

Pyridine (py) complexes of the general formula *trans*-$[M(py)_4X_2]^{n+}$, M being a divalent or trivalent metal ion and X some monodentate ligand, are known for almost all transition metal ions exhibiting a classical coordination chemistry. Since these compounds are generally relatively easy to prepare, several studies concerning their structure and also their chemical and physical properties have appeared in the literature. Because of our general interest in coordination compounds having the electronic configuration d^3 and the lack of any ESR characterizations of a series of analogous V^{II} coordination compounds we decided to investigate the *trans*-$V^{II}(py)_4X_2$ system. This series was chosen because it allows a comparison of the spin-Hamiltonian parameters with those of the analogous and isoelectronic chromium(III) compounds. At the same time we found that the *trans*-$Mn^{II}(py)_4X_2$ series had not been characterized by means of ESR spectroscopy, and therefore these have been included in the present study. This also opens up the possibility of comparing spin-Hamiltonian parameters of analogous compounds having different electronic configurations.

Experimental Section

All operations involving vanadium(II), ruthenium(II), and iron(II) compounds were carried out in an protective atmosphere of dinitrogen using Schlenk equipment and standard vacuum techniques. The chemicals used were at least of reagent grade and used without further purification.

Synthesis. *trans*-$V(py)_4X_2$[1] (X = Cl, Br, I), *trans*-$V(py)_4(NCS)_2$,[2] *trans*-$Ru(py)_4Cl_2$,[3,4] *trans*-$M^{II}(py)_4(NCS)_2$[5] (M^{II} = Mn, Fe, Co, Ni), and *trans*-$M^{II}(py)_4Cl_2$[6] (M^{II} = Fe, Ni) were prepared according to the published procedures. *trans*-$Mn(py)_4X_2$ (X = Cl, Br, I), *trans*-$Co(py)_4X_2$ (X = Cl, Br) and *trans*-$Fe(py)_4X_2$ (X = Br, I), which have all been thoroughly described in the literature, were obtained by refluxing the appropriate hydrated halide in an excess of pyridine until the temperature reached 119 °C. It is important to eliminate all the water from the reaction mixture; otherwise, the compounds are contaminated with variable amounts of hydrates. Subsequent cooling and filtration yielded the respective compounds in almost quantitative yields. *trans*-$Ru(py)_4Br_2$ were prepared by a procedure analogous to that of *trans*-$Ru(py)_4Cl_2$[4] using $RuBr_3 \cdot xH_2O$ as a starting material. The compound was obtained in approximately the same yield as *trans*-$Ru(py)_4Cl_2$ and gave satisfactory elemental analyses. All the above-mentioned compounds were recrystallized from boiling pyridine.

Properties of the Compounds. All the *trans*-$V(py)_4X_2$ (X = NCS, Cl, Br, I) compounds have intense red-brown colors. They are oxidized rapidly by contact with atmospheric dioxygen but somewhat slower if thoroughly dried. The *trans*-$Co(py)_4X_2$ (X = NCS, Cl, Br) compounds are red-violet and only stable for longer periods in an atmosphere of pyridine. Exposure to air rapidly led to the loss of pyridine yielding the intensely blue polymeric $Co(py)_2X_2$. Refluxing $CoI_2(aq)$ in an excess of pyridine yields the green $[Co(py)_6]I_2$. *trans*-$Ru(py)_4X_2$ (X = Cl, Br) are obtained as large red-brown crystals when allowed to crystallize slowly from pyridine.

[†] University of Copenhagen.

[‡] Haldor Topsøe A/S.

[§] These results have been presented in a preliminary form at the 29th ICCC 1992, Lausanne, Switzerland.

(1) Khamar, M. M.; Larkworthy, L. F.; Patel, K. C.; Phillips, D. J.; Beech, G. *Aust. J. Chem.* **1974**, *27*, 41.

(2) Larkworthy, L. F.; Tucker, B. J. *Inorg. Chim. Acta* **1978**, *33*, 167.

(3) Gilbert, J. D.; Rose, D.; Wilkinson, G. *J. Chem. Soc. A* **1970**, 2765.

(4) Evans, I. P.; Spencer, A.; Wilkinson, G. *J. Chem. Soc., Dalton Trans.* **1973**, 204.

(5) Kauffman, G. B.; Albers, R. A.; Harlan, F. R. *Inorg. Synth.* **1970**, *12*, 251.

(6) Long, G. J.; Clarke, P. J. *Inorg. Chem.* **1978**, *17*, 1394.

0020-1669/93/1332-1216\$04.00/0

Table I. Space Groups and Cell Parameters of *trans*-$M^{II}(py)_4X_2$

X	param	M = V	M = Mn	M = Fe	M = Co	M = Ni	M = Ru
NCS	space group[a]	*C*2/*c*[b]	*C*2/*c*[b]	*C*2/*c*[16]	*C*2/*c*[14]	*C*2/*c*[17]	
	a/Å	12.394(5)	12.522(4)	12.25(1)	12.461(6)	12.434(4)	
	b/Å	13.118(6)	13.180(4)	13.18(1)	12.910(6)	12.944(5)	
	c/Å	16.393(6)	16.590(5)	16.46(1)	16.509(8)	16.461(6)	
	β/deg	118.09(4)	118.67(30)	117.9(1)	118.60(5)	118.78(2)	
	Z	4	4	4	4	4	
Cl	space group	$I4_1/acd$[11]		$I4_1/acd$[6]	$I4_1/acd$[6]	$I4_1/acd$[b]	$I4_1/acd$[b]
	a/Å	15.902(6)		15.945(2)	15.996(2)	15.939(5)	15.675(2)
	b/Å	17.105(6)		17.287(6)	17.153(6)	17.084(9)	16.997(3)
	Z	8		8	8	8	8
Br	space group	$Pmn2_1$ or[b] *Pmnm*	$Pmn2_1$ or[b] *Pmnm*	$Pna2_1$[b]	$Pna2_1$[15]	$Pna2_1$[b]	*Fddd*[b]
	a/Å	13.013(7)	13.079(5)	16.117(6)	15.9(1)	15.951(3)	21.751(5)
	b/Å	9.174(3)	9.194(5)	9.513(3)	9.5(1)	9.453(2)	23.583(5)
	c/Å	17.274(7)	17.342(5)	14.277(9)	14.2(1)	14.133(4)	16.876(5)
	Z	4	4	4	4	4	16
I	space group		*Pbcn*[b]	*Pbcn*[b]		*Pbcn*[18]	
	a/Å		9.807(10)	9.776(5)		9.678(4)	
	b/Å		16.303(10)	16.212(5)		16.077(6)	
	c/Å		14.181(10)	14.131(7)		14.004(4)	
	Z		4	4		4	

[a] From the XRPD data it is not possible to distinguish between the space groups *C*2/*c* or *Cc*. *C*2/*c* is assumed from isomorphism with Fe,[16] Co,[14] and Ni[17] compounds. [b] This work. Data obtained at room temperature.

XRPD clearly demonstrates that the product obtained by the reaction of *trans*-$Ru(DMSO)_4Cl_2$ with pyridine is identical to that obtained by addition of pyridine to the blue ruthenium(II) chloride solution of Wilkinson.[3] When the crystals are crushed in a mortar or precipitated very quickly, a fine yellow microcrystalline powder results. The two ruthenium(II) compounds are both stable for at least several months when exposed to the atmosphere. The thiocyanato complex could not be prepared by refluxing $K_3Ru(NCS)_6$ in DMSO and thereupon refluxing the obtained bright yellow precipitate in pyridine. *trans*-$Fe(py)_4X_2$ (X = NCS, Cl, Br, I) are all yellow compounds. They are only stable for longer periods when stored under dinitrogen. Cell parameters obtained from X-ray powder diffraction of most of the compounds are shown in Table I.

ESR Spectra. Samples appropriate for recording ESR spectra were obtained by dissolving the solid solvent in boiling pyridine and subsequently adding approximately 1% of the vanadium(II) or manganese(II) compounds. When all had dissolved the solution was filtered and quickly chilled in an ice bath. In this way a finely crystalline powder immediately suited for ESR measurements was obtained and separated by filtration. The vanadium and manganese contents were not analyzed.

Powdered samples containing vanadium(II) were transfered to ESR tubes and measured under dinitrogen. It was not possible, however, to exclude traces of dioxygen. All ESR spectra were recorded with a Bruker ESP spectrometer equipped with an Oxford ESR-900 continuous-flow cryostat. The spectra were obtained at the X-band (9.37 GHz) using a modulation frequency of 100 kHz and amplitudes between 5–10 G and therefore as usual appear as first derivatives of absorptions. The magnetic field range was 50–15050 G.

Simulation of ESR Spectra. The simulation program[7] calculates the ESR spectra according to the formula

$$I(H) = \sum\nolimits_\beta \sum\nolimits_\gamma \Big[\sum_{i=1}^{N(\beta,\gamma)} P_i F_i(H_i,\Gamma_i;H) \Big] \Delta\beta\Delta\gamma \qquad (1)$$

which is a simple addition of single crystal spectra. $N(\beta,\gamma)$ is the number of transitions to be searched for each orientation of the magnetic field with respect to the molecular coordinate system. The orientation of the magnetic field vector is specified by the two Euler angles β and γ. H_i is the resonant magnetic field and P_i is the transition probability for the *i*th transition. P_i is integrated over the third Euler angle α, which is not explicitly written in (1). $F_i(H_i,\Gamma_i;H)$ is a band shape function centered at the resonant magnetic field H_i with the half-width Γ_i in half-height. All spectra were computed with Lorentzian derivative shape functions with Γ_i in the range 15–40 G (constant in each spectrum).

A precise description of the simulation algorithm will be described elsewhere.[7] We should mention here, however, that the resonant magnetic fields are found by numerical diagonalization of the spin-Hamiltonian matrix which is of dimension 36 (72) and 32 (64) for manganese(II) and vanadium(II), respectively. The numbers in parentheses apply to the nonaxial cases as we expand the matrices instead of using a diagonalization routine for complex matrices.

No selection rules were included in the search for transitions. Thus 540 and 384 transitions were searched for each orientation of the magnetic field for manganese(II) and vanadium(II), respectively. Depending primarily on the size of the zero-field splitting (zfs) parameters *D* and *E*, β and γ were varied in steps of 0.5–2 and 2–10°, respectively.

All spectra were calculated on an IBM RS/6000-320H computer and typical CPU time was about 30 min for the axial cases and about 10 h for the nonaxial ones.

X-ray Powder Diffraction. (XRPD) X-ray powder diagrams of the compounds were recorded at room temperature by slow scanning on a Philips vertical goniometer equipped with a θ-compensating divergence slit and a diffracted beam graphite monochromator utilizing Cu $K\text{-}L_{2,3}$ radiation (IUPAC recommended designation for Cu Kα radiation[8]). Indexing of the powder patterns was made either by comparison with isomorphous compounds or by utilizing the software supplied by the manufacturers, based on the program by Visser.[9] When these attempts failed, solutions were found from scrutiny of $1/d^2$ values. Cell parameters were refined by least-squares refinement.

Results

Structures. Many of the compounds studied have previously been characterized by single-crystal and/or powder X-ray diffraction. The results of these investigations together with our new results are summarized in Table I. As seen from this table the space groups seem to be determined primarily by the anion rather than by the central metal ion. Altogether this results in four anion series, the compounds within three of these being isomorphous, having almost identical cell parameters, and therefore perfectly suited for our dilution experiments. Only the compounds in the bromo series are not isomorphous, and certainly *trans*-$Ru^{II}(py)_4Br_2$ is conspicuous. Here it is to be noted that all the compounds investigated by single-crystal X-ray diffraction crystallize in space groups having the metal ions in general positions with nonaxial site-symmetries as illustrated in Figure 1, where schematic representations of *trans*-$Co(py)_4(NCS)_2$ and *trans*-$Co(py)_4Cl_2$ are shown. These compounds are typical of all those investigated. Consequently all the bis(thiocyanato-*N*) complexes have C_i symmetry and the pyridines opposite to each other are approximately coplanar. The dichloro-, dibromo-, and diiodotetrakis(pyridine) complexes have the pyridines coordinated

---

(7) Glerup, J.; Weihe, H. To be submitted to *J. Magn. Reson.*

(8) *Pure Appl. Chem.* **1991**, *63*, 736.

(9) Visser, J. *J. Appl. Crystallogr.* **1969**, *2*, 85.

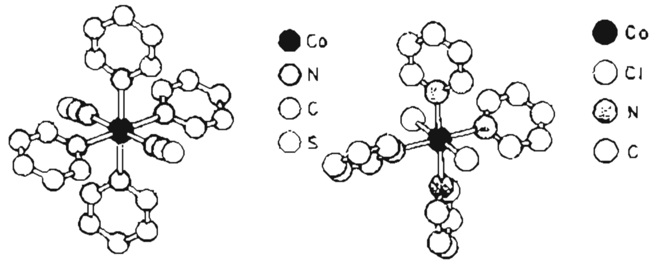

Figure 1. Schematic representation of the structures of *trans*-Co(py)$_4$(NCS)$_2$ (left) and *trans*-Co(py)$_4$Cl$_2$ (right) illustrating the two different modes of pyridine coordination.

in a propeller-like arrangement which ideally has C_4 symmetry. Slight deviations from this ideal symmetry are observed, however, resulting in the chloro and bromo complexes only having D_2 symmetry and the iodo complexes only C_2 symmetry. These considerations, of course, only apply to the compounds investigated by single-crystal X-ray diffraction. The XRPD data, however, in most cases suggest similar structures within each anion series.

Determination of Spin-Hamiltonian Parameters. Generally, the ESR spectra of crystalline powders can be recorded more simply than those of single crystals. Since the vanadium(II) compounds, as mentioned, are very sensitive to oxidation by atmospheric dioxygen, we did not make any attempts to grow single crystals. All spin-Hamiltonian parameters reported in this paper are thus extracted from powder spectra and are obtained by the described simulation procedure.

The spectra could be interpreted in terms of the conventional spin-Hamiltonian

$$\hat{H} = \mu_B \mathbf{H}\cdot\mathbf{g}\cdot\hat{\mathbf{S}} + \hat{\mathbf{S}}\cdot\mathbf{A}\cdot\hat{\mathbf{I}} + D[\hat{S}_z^{\,2} - {}^1/_3 S(S+1)] + E[\hat{S}_x^{\,2} - \hat{S}_y^{\,2}] + {}^1/_6 a[\hat{S}_x^{\,4} + \hat{S}_y^{\,4} + \hat{S}_z^{\,4}] = \mu_B[g_x H_x \hat{S}_x + g_y H_y \hat{S}_y + g_z H_z \hat{S}_z] + D[\hat{S}_z^{\,2} - {}^1/_3 S(S+1)] + E[\hat{S}_x^{\,2} - \hat{S}_y^{\,2}] + {}^1/_6 a[\hat{S}_x^{\,4} + \hat{S}_y^{\,4} + \hat{S}_z^{\,4}] + A_x \hat{S}_x \hat{I}_x + A_y \hat{S}_y \hat{I}_y + A_z \hat{S}_z \hat{I}_z \quad (2)$$

with $(S, I) = ({}^3/_2, {}^7/_2)$ for vanadium(II) and $(S, I) = ({}^5/_2, {}^5/_2)$ for manganese(II) and all the parameters having their usual meanings. As seen from our spin-Hamiltonian (2), we have assumed that the principal axes of the **g** tensor and the **A** tensor are parallel. From the powder spectra it is, in principle at least, possible to determine the relative orientations of these two principal coordinate systems. In practice, however, this is by no means an easy task when both tensors are as close to being isotropic as in the present case. On the other hand the very small anisotropy indicates that even if the principal axes of the **g** tensor and the **A** tensor are not parallel (2) will still be a satisfactory Hamiltonian.

In the analysis of the manganese(II) spectra we first neglected the fourth-order spin operator terms but included them at later stages of the analysis when this resulted in a better fit. These parameters can, however, only be regarded as first approximations. Our simulation procedure does not make any approximations and every term in (2) is thus fully accounted for.

Initial values of g_x, g_y, g_z, D, and E were obtained by calculating spectra without considering the nuclear spin. When satisfactory agreement was obtained, the nuclear spin was included and the hyperfine coupling constants estimated from the spacings between the hyperfine lines. All parameters were then adjusted until most of the hyperfine lines were satisfactorily accounted for. We have not determined the signs of the zero-field splittings, and only the numerical values of the hyperfine coupling constants have been obtained. We estimate that the g values are accurate to within 0.1% and the rest of the spin-Hamiltonian parameters to within 0.5%. The only exception to this is the spin-Hamiltonian parameters of *trans*-Mn(py)$_4$(NCS)$_2$ which we have not been able to obtain with this high accuracy since the zfs is very small and the spectra in this region of the zfs range are very similar.

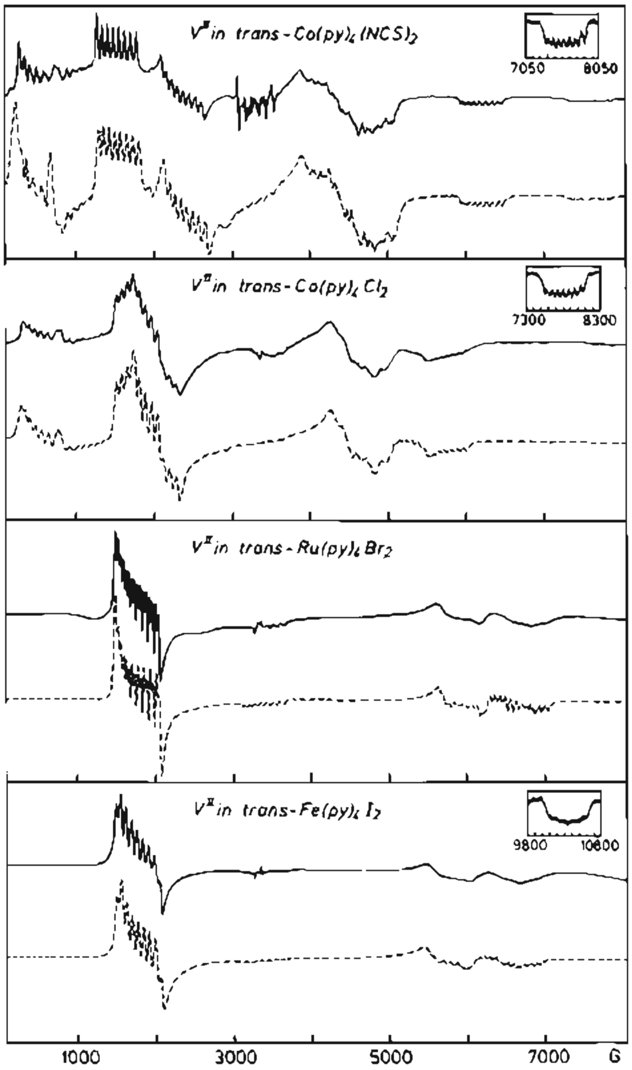

Figure 2. Experimental (—) and simulated (- -) ESR spectra of 1% V^{II} in *trans*-Co(py)$_4$(NCS)$_2$, *trans*-Co(py)$_4$Cl$_2$, *trans*-Ru(py)$_4$Br$_2$, and *trans*-Fe(py)$_4$I$_2$. All spectra were recorded at room temperature using a microwave frequency of 9.37 GHz and a modulation field of frequency 100 kHz and amplitude of 5 G. The microwave power was 20 mW.

Description of the Spectra. The ESR spectra of the *trans*-V^{II}(py)$_4$X$_2$ series are shown in Figure 2 together with the spectra simulated from the spin-Hamiltonian parameters given in Table II. We have chosen to illustrate the effect of using the diamagnetic ruthenium(II) as well as the paramagnetic cobalt(II) and iron(II) compounds as solid solvents. As apparent from the results shown in Table II the zero-field splittings are almost independent of the solid solvent. The most pronounced exception to this is observed when *trans*-Ru(py)$_4$Br$_2$ is used as solid solvent. This might be related to the different structure of this compound as the same trend is observed for Mn^{II} in *trans*-Ru(py)$_4$Br$_2$. We have also recorded the spectra of the pure V^{II} compounds. These were characterized by having broader lines leaving all hyperfine structure unresolved. The fine structure was, however, resolved relatively well, and approximately the same spin-Hamiltonian parameters as those of the diluted samples could be obtained. Since it was not possible completely to exclude dioxygen and since the vanadium(II) compounds are generally very susceptible to oxidation, the spectra contain signals in the region around $g \sim 2$ that are due to the thereby introduced trace impurities. This has been proved by measuring the spectra without the protective atmosphere of dinitrogen and thereupon observing a steadily increasing intensity of the spectrum around $g \sim 2$ relative to that

Table II. Spin-Hamiltonian Parameters for *trans*-$V^{II}(py)_4X_2$[a]

	T/K	g_x	g_y	g_z	D/cm^{-1}	E/cm^{-1}	10^4A_x/cm^{-1}	10^4A_y/cm^{-1}	10^4A_z/cm^{-1}
V^{II} in $Co^{II}(py)_4(NCS)_2$	298	1.9855	1.9855	1.9850	0.1941	0.0253	68	$68._5$	70
V^{II} in $Fe^{II}(py)_4(NCS)_2$	298	1.985	1.985	1.985	0.193	0.025	68	68	70
V^{II} in $Co^{II}(py)_4Cl_2$	298	1.985	1.985	1.987	0.205	0.0078	70	70	70
V^{II} in $Fe^{II}(py)_4Cl_2$	298	1.985	1.985	1.985	0.205	0.009	70	70	70
V^{II} in $Ru^{II}(py)_4Cl_2$	298	1.985	1.985	1.982	0.208	0	70	70	68
V^{II} in $Ru^{II}(py)_4Cl_2$	80	1.985	1.985	1.985	0.209	0.0035	70	70	70
V^{II} in $Co^{II}(py)_4Br_2$	298	1.985	1.985	1.985	0.295	0.007	70	70	70
V^{II} in $Fe^{II}(py)_4Br_2$	298	1.986	1.986	1.986	0.293	0.0083	68	68	70
V^{II} in $Ru^{II}(py)_4Br_2$	298	1.985	1.985	1.986	0.338	0.0032	69	69	70
V^{II} in $Ru^{II}(py)_4Br_2$	80	1.986	1.986	1.990	0.352	0.0040	67	67	70
V^{II} in $Fe^{II}(py)_4I_2$	298	1.989	1.989	1.989	0.372	0.0046	66	66	69

[a] All spectra were simulated using band widths in the range 20–40 G.

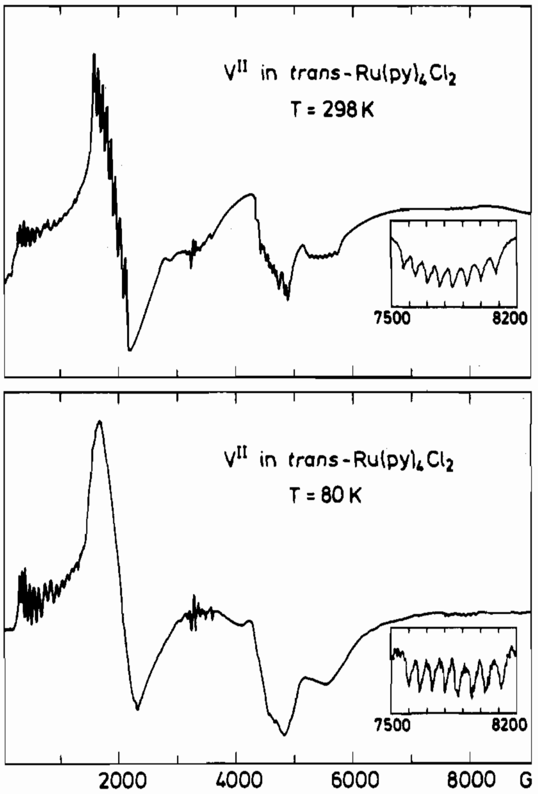

Figure 3. ESR spectra of 1% V^{II} in *trans*-$Ru(py)_4Cl_2$ at 298 and 80 K. From these spectra it is evident that the coordination environment of V^{II} changes from axial at room temperature to nonaxial at 80 K. The spectra were obtained with the spectrometer settings used in Figure 2.

of the *trans*-$V^{II}(py)_4X_2$. We have not in any way attempted to identify the oxidation products but only note that their ESR spectra are characteristic of VO^{2+} compounds. Furthermore, a signal very close to $g \sim 2$ is observed in the spectra. This has been ascribed to an impurity in the cavity as the signal has also been observed from a blank sample.

Figure 3 illustrates the spectra of *trans*-$V(py)_4Cl_2$ diluted in *trans*-$Ru(py)_4Cl_4$ measured at 298 and 80 K. The pronounced difference between the two spectra is ascribed to a reversible phase transition of the *trans*-$Ru(py)_4Cl_2$, the transition apparently taking place well above 150 K. We found that the space group was still $I4_1/acd$ down to 110 K (found by a single-crystal measureasurement on a four-circle diffractometer) and the cell parameters almost unchanged. We suggest, therefore, that at room temperature the Ru^{II} species are located in the general positions having 4-fold symmetry and this changes to D_2 symmetry at lower temperatures as it is possible in the space group $I4_1/acd$. An analogous difference is observed for *trans*-$Mn(py)_4Cl_2$ diluted in *trans*-$Ru(py)_4Cl_2$. The phase transition shifts the magnitude of the zfs much more for manganese(II) than for vanadium(II). As is apparent from the spin-Hamiltonian parameters given in Table II, the zfs of *trans*-$V(py)_4(NCS)_2$ and *trans*-$V(py)_4Cl_2$ are almost identical and are close to 0.4 cm^{-1}. The zfs of *trans*-$V(py)_4Br_2$ and *trans*-$V(py)_4I_2$ are also rather similar (somewhat dependent upon the solid solvent) with a value around 0.75 cm^{-1}. If, however, a comparison is made between the spin-Hamiltonian parameters of V^{II} diluted in the *trans*-$Fe^{II}(py)_4X_2$ series, it is evident that the iodo complex has a higher zfs than the bromo complex.

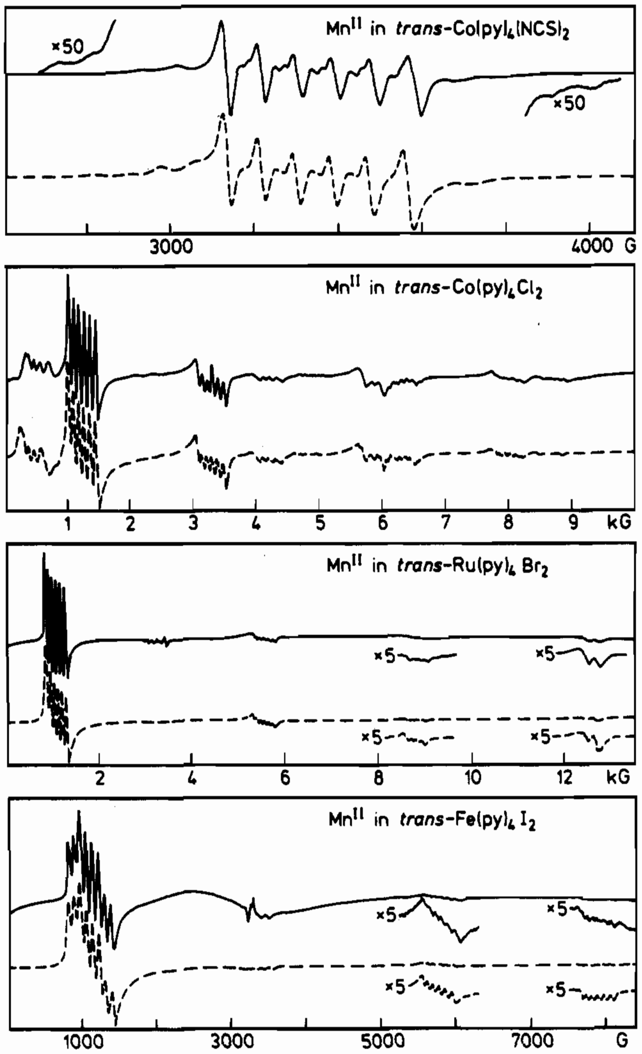

Figure 4. Experimental (—) and simulated (- -) ESR spectra of 1% Mn^{II} in *trans*-$Co(py)_4(NCS)_2$, *trans*-$Co(py)_4Cl_2$, *trans*-$Ru(py)_4Br_2$, and *trans*-$Fe(py)_4I_2$. All spectra were recorded at room temperature. Different portions of the four spectra have been shown in order to emphasize all the dominant features of each spectrum. Note that the spectra shown have been obtained using the same solid solvents as in Figure 2. The spectrometer settings were as those of the V^{II} spectra in Figure 2.

In Figure 4 the ESR spectra of the four *trans*-$Mn^{II}(py)_4X_2$ (X = NCS, Cl, Br, I) compounds are shown together with the spectra simulated from the spin-Hamiltonian parameters given in Table

Table III. Spin-Hamiltonian Parameters for *trans*-$Mn^{II}(py)_4X_2$[a]

	T/K	g_{iso}	D/cm^{-1}	E/cm^{-1}	10^4A_{iso}/cm^{-1}	a/cm^{-1}
Mn^{II} in $Co^{II}(py)_4(NCS)_2$	298	2.00	~0.01	~0.002	80	~0.0005
Mn^{II} in $Fe^{II}(py)_4(NCS)_2$	298	2.00	~0.01	-0.003	80	~0.000
Mn^{II} in $Co^{II}(py)_4Cl_2$	298	2.00	0.208	0.000	77	0.002
Mn^{II} in $Ru^{II}(py)_4Cl_2$	298	2.00	0.2195	<0.0001	77	0.002
Mn^{II} in $Ru^{II}(py)_4Cl_2$	80	2.00	0.256	0.0014	77	0.002
Mn^{II} in $Co^{II}(py)_4Br_2$	298	2.00	0.590	0.0032	77	0
Mn^{II} in $Fe^{II}(py)_4Br_2$	298	2.00	0.586	0.0030	77	0
Mn^{II} in $Ru^{II}(py)_4Br_2$	298	2.00	0.665	0.0007	77	0.002
Mn^{II} in $Ru^{II}(py)_4Br_2$	80	2.00	0.717	0.0008	77	0
Mn^{II} in $Fe^{II}(py)_4I_2$	298	2.00	0.932	0.0196	77	0

[a] All Mn^{II} spectra were simulated using isotropic g and A values. Bandwidths used were in the range 15–30 G.

III. It has been necessary to illustrate different portions of the spectra to be able to emphasize all the important features of the individual spectra. Here a development in the zfs parameters quite different from that of the *trans*-$V(py)_4X_2$ system is observed. *trans*-$Mn(py)_4(NCS)_2$ appears to be almost cubic having only a very small zfs. The zfs of the other three compounds increases in a regular stepwise fashion from *trans*-$Mn(py)_4Cl_2$ via *trans*-$Mn(py)_4Br_2$ to *trans*-$Mn(py)_4I_2$. It has been generally found that the zfs of the *trans*-$Mn(py)_4X_2$ compounds are larger than those previously reported for the corresponding *trans*-Mn(γ-picoline)$_4X_2$ compounds.[10]

Discussion

Very few ESR spectra of vanadium(II) compounds have appeared in the literature, and the present study is the first in which an investigation of a series of analogous V^{II} compounds is undertaken. Therefore we will shortly discuss some of the properties of vanadium(II) compounds that are relevant to the measurement and interpretation of the ESR spectra.

The naturally occurring vanadium consists primarily of two isotopes of which ^{51}V is by far the dominant one (99.75%). This nuclide has a nuclear spin ($I_v = {}^7/_2$) and a nuclear magnetic moment of 5.139 μ_N (compared to –0.4735 μ_N for ^{53}Cr (9.55%)) which is part of the reason why the hyperfine structure is frequently well resolved. Vanadium(II) has the electronic configuration d^3 and is, therefore, isoelectronic with the much more studied chromium(III). The ground state is thus a spin quartet and as the ratio ζ/Δ_o, ζ being the spin–orbit coupling constant and Δ_o the octahedral ligand-field parameter, is not very different for vanadium(II) and chromium(III) ($\zeta_{V(II)} = 167$ cm^{-1} and $\zeta_{Cr(III)} = 274$ cm^{-1} for the free ions) the ESR spectra of vanadium(II) are expected to be easily obtained. This is so, because the information given above indicates that vanadium(II) will have excited states with mean life times favorable with respect to ESR measurements just as it is empirically the case for chromium(III). From this discussion the ESR spectra of vanadium(II) would generally be assumed to be quite similar to those of chromium(III) apart from the fact that each fine structure line is split because of the nuclear spin.

One of the purposes of this investigation has been to compare the spin-Hamiltonian parameters of analogous vanadium(II) and chromium(III) compounds. The *trans*-$V(py)_4Cl_2$ and *trans*-$Cr(py)_4X_2^+$ series are, as mentioned, isoelectronic. However, to make the comparison, another important question is whether the two series have similar structures. Here a complication arises as none of the *trans*-$Cr(py)_4X_2^+$ compounds have had their structures elucidated by single-crystal X-ray diffraction. *trans*-$V(py)_4Cl_2$ has,[11] however, as have several of the solid solvents used in this study, and as these are isomorphous with the vanadium(II) compounds a reasonable assumption would be that the V^{II} is situated in a site with C_i, D_2, and C_2 symmetry in the thiocyanato-*N*, chloro (and bromo), and iodo complexes, respectively. The *trans*-$Cr(py)_4X_2^+$ compounds were in the work of Pedersen and Toftlund[12] diluted in the analogous rhodium(III) compounds of which *trans*-[$Rh(py)_4BrCl$]Cl has been examined by means of single-crystal X-ray diffraction and thereby shown to have the Rh^{III} in a site with C_4 symmetry,[13] i.e. with the pyridine coordinated in a propeller-like arrangement. The chromium(III) complexes were, however, found in several cases to have a nonzero zfs parameter E, indicating a nonaxial coordination geometry. Furthermore, V^{II} diluted in *trans*-$Ru(py)_4Cl_2$ appears to be situated in an axially symmetric environment at room temperature and in a nonaxially symmetric environment at liquid nitrogen temperature (Figure 3) just as it is the case for Mn^{II} in *trans*-$Ru(py)_4Cl_2$. This situation makes a comparison of the zfs parameters D and E individually rather meaningless. Therefore we will only discuss the total zero-field splittings given by $2(D^2 + 3E^2)^{1/2}$. At this point it is important to note that the following discussion only concerns the size of the zfs and not the sign (i.e. whether the $\pm{}^3/_2$ or the $\pm{}^1/_2$ state has the lowest energy at zero magnetic field remains unresolved). In the *trans*-$V(py)_4X_2$ series, it has been mentioned that the zfs of *trans*-$V(py)_4(NCS)_2$ and *trans*-$V(py)_4Cl_2$ are almost identical just as those of *trans*-$V(py)_4Br_2$ and *trans*-$V(py)_4I_2$ are very similar. Contrary to this the zfs rapidly increases from *trans*-$Cr(py)_4Cl_2^+$ via *trans*-$Cr(py)_4Br_2^+$ to *trans*-$Cr(py)_4I_2^+$ (the bis(thiocyanato-*N*) complex is unknown) in a regular way. This trend is the one expected from the second order perturbation expression for the zfs parameter D in tetragonal symmetry

$$D = \frac{8\zeta^2[E(^4B_2) - E(^4E)]}{9\Delta_{av}^2}$$

where ζ is the spin-orbit coupling constant, Δ_{av} the octahedral ligand-field parameter and $E(^4B_2)$ and $E(^4E)$ are the energies of the tetragonal split components of the $^4T_2(O_h)$ term. However, in the case of chromium(III) it was necessary in qualitative terms to introduce the possibility of chromium "borrowing" the spin-orbit coupling constant from the halide ligands in order to obtain a satisfactory correlation between the ligand-field calculations based upon the UV–vis spectra and the observed zero-field splittings.[12] In the case of the V^{II} compounds the UV–vis spectra are not yet well understood,[1] leaving the discussion open. In this respect it might be important that superhyperfine coupling to the heavy halide ligands is observed for chromium(III) but not for vanadium(II). The g values for the V^{II} complexes are very close to those previously reported for the *trans*-$Cr(py)_4X_2^+$ compounds,

---

(10) Dowsing, P. D.; Gibson, J. F.; Goodgame, M.; Hayward, P. J. *J. Chem. Soc. A* **1969**, 187.

(11) Brauer, D. J.; Krüger, C. *Cryst. Struct. Commun.* **1973**, *3*, 421.

(12) Pedersen, E.; Toftlund, H. *Inorg. Chem.* **1974**, *13*, 1603.

(13) Pedersen, E.; Toftlund, H.; Watson, K. J.; Yde-Andersen, S. Unpublished results.

(14) Hartl, H.; Brüdgam, I. *Acta Crystallogr.* **1980**, *B36*, 162.

(15) Anciškina, A. C.; Poraj-Košic, M. A. *Kristallografija* **1958**, *3*, 676.

(16) Søtofte, I.; Rasmussen, S. E. *Acta. Chem. Scand.* **1967**, *21*, 2028.

(17) Valach, F.; Sivý, P.; Koreň, B. *Cryst. Struct. Commun.* **1973**, *C46*, 957.

(18) Hamm, D. J.; Bordner, J.; Schneider, A. F. *Inorg. Chim. Acta* **1973**, *7*, 637.

and this is to be expected upon consideration of the second-order perturbation expression

$$g = 2 - \frac{8\zeta}{3\Delta}$$

which suggests very similar values for analogous compounds of chromium(III) and vanadium(II). Considering the simplicity of this calculation, the agreement can be considered satisfactory.

The *trans*-$Mn(py)_4X_2$ series have spin-Hamiltonian parameters which exhibit trends similar to those of the Cr^{III} system. Comparison of Figures 2 and 3 (or alternatively Tables II and III) convincingly illustrates that the ratio of E to D is larger for *trans*-$V(py)_4Cl_2$ and *trans*-$V(py)_4Br_2$ than for *trans*-$Mn(py)_4Cl_2$ and *trans*-$Mn(py)_4Br_2$, respectively. The opposite situation is found for the thiocyanato-*N* and iodo complexes, as E/D is larger for *trans*-$Mn(py)_4(NCS)_2$ and *trans*-$Mn(py)_4I_2$ than for *trans*-$V(py)_4(NCS)_2$ and *trans*-$V(py)_4I_2$, respectively. It is worth noticing that this comparison applies to compounds diluted in the same solid solvent, and this situation emphasizes the complex nature of the zfs.

The use of the paramagnetic Co^{II} and Fe^{II} compounds as solid solvents is rather unusual. A few examples of this are found in the literature, and their applicability is ascribed to their orbitally degenerate ground states causing very short relaxation times. We have in this respect found that the spectra obtained using the *trans*-$Ni(py)_4X_2$ as solid hosts are very similar to those obtained from the undiluted V^{II} and Mn^{II} compounds. Therefore, this can probably be related to the orbitally nondegenerate ground state of Ni^{II}.

Conclusion

It has been possible to obtain the spin-Hamiltonian parameters of all the *trans*-$V^{II}(py)_4X_2$ and *trans*-$Mn^{II}(py)_4X_2$ compounds, and in most cases the influence of the solid solvent on the parameters has been investigated by using several hosts, diamagnetic as well as paramagnetic. The parameters of V^{II} have been compared to those of the analogous and isoelectronic chromium(III) compounds. It has, however, not been possible to find any simple correlations. The dependence of the zfs upon X of the *trans*-$V(py)_4X_2$ series can be summarized by

$$NCS^- \approx Cl^- < Br^- \approx I^-$$

compared to the analogous chromium(III) series

$$Cl^- < Br^- < I^-$$

which is very similar to that of the manganese(II) series

$$NCS^- < Cl^- < Br^- < I^-$$

Before a more quantitative treatment of the spin-Hamiltonian parameters reported in this paper can be undertaken a more rigorous analysis of the UV–vis spectra of *trans*-$V^{II}(py)_4X_2$ has to be made. This analysis will probably be complicated by the intense charge transfer band in the visible region of the vanadium(II) spectra.[1]

Acknowledgment. We are indebted to H. Toftlund for valuable discussions concerning the comparison of the V^{II} and Cr^{III} ESR spectra and to F. Hansen for carrying out the single-crystal diffraction experiment.